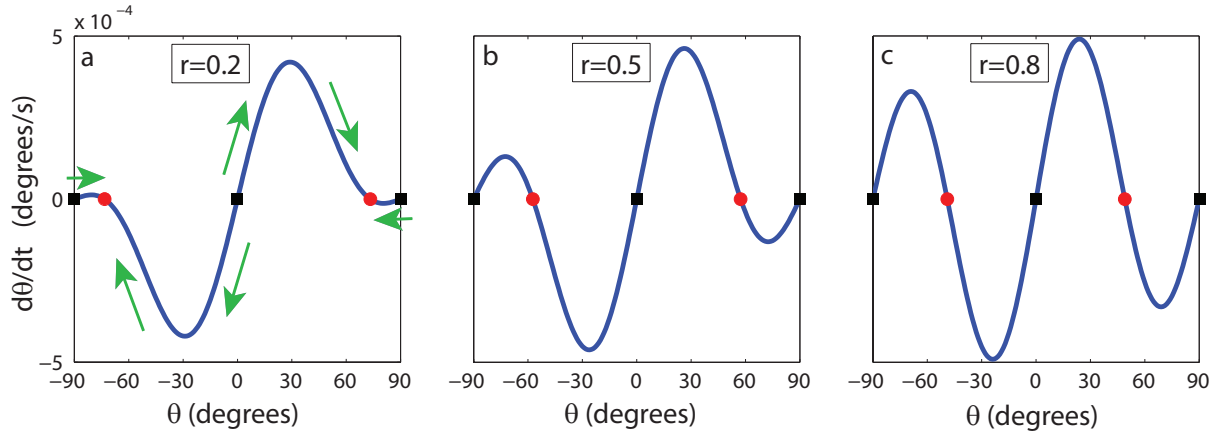


**Supplementary Figure 1. Cell, SF and FA co-alignment following cyclic stretching.** **a**, SFs (red) and FAs (yellow) in a single cell after 6 hours of cyclic stretching. The REF-52 cell, expressing YFP-tagged paxillin (FA protein), was fixed at the end of the stretch and stained with TRITC-phalloidin. **a'**, Blowup of (a) demonstrates that the SFs are orientated at a similar angle. A further magnification shows that FAs are co-aligned with the SFs anchored to them. The sketch, of a single FA (yellow) - SF (red) pair, illustrates the joint orientation angle,  $\theta$ , as well as their polarization direction,  $\rho$ . In comparison, the substrate extensional principal strain is in the direction of the  $x$  axis (this usually, but not always, coincides with the direction of applied stretching). **b**, Images of single REF-52 cells (one nucleus each), after 6 hours of cyclic stretching, showing SFs oriented at both mirror-image angles. This result indicates that the reorientation is not driven at the cell level, but rather involves a smaller part of it. Such mixed orientations are typically observed in cells originally aligned perpendicular to the direction of the extensional principal strain (i.e. midway between the two mirror-image angles) and can be explained by SF clusters reorienting independently towards the closer set point angle (see Fig. 4b).



**Supplementary Figure 2.** Plots of  $\frac{d\theta}{dt}$  for different  $r$  values. **a**,  $r = 0.2$ . **b**,  $r = 0.5$ . **c**,  $r = 0.8$ . Red circles mark the steady state solutions (predicted final orientations), black squares mark the unstable fixed-points and green arrows (only in (a)) indicate the reorientation directions. For all plots,  $\check{\varepsilon}_{xx} = 0.1$ ,  $b = 1.13$  and  $\tau = 6.6$  sec were used.

### Supplementary Note 1: Reorientation under cyclic stretching is driven by dissipative relaxation of the cell's passively-stored, two-dimensional, elastic energy

Here we lay out a new theory which accurately captures the dynamics of stress fibres (SFs), focal adhesions (FAs) and cell reorientation under cyclic stretching. The constraints and thresholds for this effect are discussed in the next section.

Biaxial cyclic stretching is applied to a  $2D$  elastic substrate, to which cells adhere. The resulting linear elastic principal strains in the substrate are

$$\varepsilon_{xx}(t) = 0.5 \cdot \check{\varepsilon}_{xx}(1 - \cos(\omega t)) \quad \text{and} \quad \varepsilon_{yy}(t) = -r \cdot \varepsilon_{xx}(t) . \quad (\text{S1})$$

$\check{\varepsilon}_{xx}$  and  $\check{\varepsilon}_{yy}$  are the time-independent strain amplitudes and  $r$  ( $-\infty < r < \infty$ ), the biaxiality strain ratio, is uniform over the region of interest.

In formulating the theory we make the following justified assumptions:

1. Cells stretch and compress together with the underlying substrate (to which they adhere). For the  $\sim 1MPa$  rigid substrate primarily used in this study, we assume that the much softer cells [1, 2] pose a negligible perturbation and inherit the matrix strains.
2. Cells should be treated as  $2D$  objects.
3. Cells should be treated as linear-elastic, anisotropic structures [2].

At the heart of the theory is the notion that the reorientation process is driven by dissipative relaxation of the cells' passively-stored, two-dimensional, elastic energy. This energy is pumped into the cells by the cyclic stretching. In response, we suggest, the cells actively and continuously realign, rotating as long as it is energetically favorable, with the final orientation angle corresponding to the elastic energy minimum.

During cyclic stretching, the elastic strain energy density stored in an individual cell,  $u^{cell}$ , is given by [3]

$$u^{cell} = \frac{1}{2}(\sigma_{\rho\rho}^{cell} \varepsilon_{\rho\rho} + \sigma_{\theta\theta}^{cell} \varepsilon_{\theta\theta} + 2\sigma_{\rho\theta}^{cell} \varepsilon_{\rho\theta}) , \quad (S2)$$

where a linear elastic relation between the matrix strains,  $\varepsilon$ , and the resulting cell stresses,  $\sigma^{cell}$ , is assumed (assumptions 1 – 2). In addition, a polar coordinate system is adopted for convenience (see Supplementary Fig. 1a'), with  $\rho$  being the direction of FAs and SFs polarization, and  $\theta$  its angle relative to the direction of the extensional principal strain (usually, but not always, the latter coincides with the direction of applied stretching). Substituting the cell stresses by their anisotropic plane-stress expressions (assumption 2)

$$\begin{aligned} \sigma_{\rho\rho}^{cell} &= \frac{1}{1 - \nu_{\theta\rho}^{cell} \nu_{\rho\theta}^{cell}} \cdot (E_{\rho\rho}^{cell} \cdot \varepsilon_{\rho\rho} + \nu_{\rho\theta}^{cell} E_{\theta\theta}^{cell} \cdot \varepsilon_{\theta\theta}) , \\ \sigma_{\theta\theta}^{cell} &= \frac{1}{1 - \nu_{\theta\rho}^{cell} \nu_{\rho\theta}^{cell}} \cdot (E_{\theta\theta}^{cell} \cdot \varepsilon_{\theta\theta} + \nu_{\theta\rho}^{cell} E_{\rho\rho}^{cell} \cdot \varepsilon_{\rho\rho}) , \\ \sigma_{\rho\theta}^{cell} &= 2\mu_{\rho\theta}^{cell} \cdot \varepsilon_{\rho\theta} , \end{aligned} \quad (S3)$$

where the cell is modeled as a linear elastic anisotropic structure (assumption 3).  $E_{\rho\rho}^{cell}$  ( $E_{\theta\theta}^{cell}$ ) is the cell Young's modulus in the  $\rho$  ( $\theta$ ) direction while  $\mu_{\rho\theta}^{cell}$  is its in-plane shear modulus.  $\nu_{\rho\theta}^{cell}$  ( $\nu_{\theta\rho}^{cell}$ ) is the cell Poisson's ratio, where stress is applied in the  $\rho$  ( $\theta$ ) direction and the lateral deformation takes place in the  $\theta$  ( $\rho$ ) direction. From the symmetric form of the stress tensor, we can reduce the number of undetermined cell elastic parameters using the following relation

$$\nu_{\rho\theta}^{cell} E_{\theta\theta}^{cell} = \nu_{\theta\rho}^{cell} E_{\rho\rho}^{cell} . \quad (S4)$$

Making use of the above equations, we obtain the following expression for the stored elastic energy density

$$u^{cell} = \frac{1}{2(1 - \nu_{\theta\rho}^{cell} \nu_{\rho\theta}^{cell})} \cdot \{ \varepsilon_{\rho\rho}^2 \cdot [E_{\rho\rho}^{cell}] + \varepsilon_{\rho\rho} \cdot \varepsilon_{\theta\theta} \cdot [2\nu_{\rho\theta}^{cell} \cdot E_{\theta\theta}^{cell}] + \varepsilon_{\theta\theta}^2 \cdot [E_{\theta\theta}^{cell}] + \varepsilon_{\rho\theta}^2 \cdot [4(1 - \nu_{\theta\rho}^{cell} \nu_{\rho\theta}^{cell}) \cdot \mu_{\rho\theta}^{cell}] \} . \quad (S5)$$

Through tensor rotation, we transform the principal strains  $\{\varepsilon_{xx}, \varepsilon_{yy}\}$  to the polar strains  $\{\varepsilon_{\rho\rho}, \varepsilon_{\theta\theta}\}$

$$\begin{aligned} \varepsilon_{\rho\rho} &= \varepsilon_{xx}[(1+r) \cdot \cos^2\theta - r] , \\ \varepsilon_{\theta\theta} &= \varepsilon_{xx}[-(1+r) \cdot \cos^2\theta + 1] , \\ \varepsilon_{\rho\theta} &= -\varepsilon_{xx}[(1+r)\cos\theta \cdot \sin\theta] . \end{aligned} \quad (S6)$$

For simplicity we rewrite Eq. S5 as

$$u^{cell} = \frac{\varepsilon_{xx}^2}{2(1 - \nu_{\theta\rho}^{cell} \nu_{\rho\theta}^{cell})} \{ (1+r)^2 \cos^4(\theta)[A+C-2(B+2D)] + 2(1+r) \cos^2(\theta)[(1+r)(B+2D)-(Ar+C)] + (Ar^2+C-2Br) \} \quad (S7)$$

where

$$\begin{aligned} A &\equiv E_{\rho\rho}^{cell} , \\ B &\equiv \nu_{\rho\theta}^{cell} \cdot E_{\theta\theta}^{cell} , \\ C &\equiv E_{\theta\theta}^{cell} , \\ D &\equiv (1 - \nu_{\theta\rho}^{cell} \nu_{\rho\theta}^{cell}) \cdot \mu_{\rho\theta}^{cell} . \end{aligned} \quad (S8)$$

This can be further simplified to the final form

$$u^{cell} = 0.5 \cdot K \cdot \varepsilon_{xx}^2 \left[ \frac{(1+r) \cdot \cos^2(\theta) - 1}{b} + (1-r) \right]^2 + f(r), \quad (S9)$$

where  $f(r)$  is a function of  $r$  with no  $\theta$  dependence and

$$b = \frac{A - (B + 2D)}{(A + C) - 2(B + 2D)},$$

$$K = \frac{1}{1 - \nu_{\theta\rho}^{cell} \nu_{\rho\theta}^{cell}} \cdot \frac{(A - (B + 2D))^2}{(A + C) - 2(B + 2D)} = \frac{b \cdot (A - (B + 2D))}{1 - \nu_{\theta\rho}^{cell} \nu_{\rho\theta}^{cell}}. \quad (S10)$$

The elastic strain energy density,  $u^{cell}$ , has two, mirror-image, stable minima for  $\theta$  at

$$\cos^2(\bar{\theta}_{theory}) = \frac{b(r-1) + 1}{r+1}, \quad (S11)$$

provided that  $K > 0$  (or  $A + C > 2(B + 2D)$ ). We then interpret these angles of minimum elastic energy,  $\bar{\theta}_{theory}$ , as the final FA and SF orientations

$$\bar{\theta}_{theory} = \pm \arccos \left( \sqrt{b + \frac{1-2b}{r+1}} \right) = \pm \arctan \left( \sqrt{\frac{r+b \cdot (1-r)}{1-b \cdot (1-r)}} \right). \quad (S12)$$

The final orientation angle is therefore a function of two parameters,  $r$  and  $b$ . The former is experimentally controlled and determined by the substrate geometry, clamping conditions and Poisson's ratio while the latter depends on the cell elastic properties.

Turning to analyze the individual cell reorientation dynamics towards  $\bar{\theta}_{theory}$ , we note that the cell inertia is negligible compared to the external elastic forces acting on it. Its reorientation, therefore, is solely driven by relaxational dynamics

$$\frac{d\theta}{dt} = -\frac{1}{\eta} \cdot \frac{\partial u^{cell}}{\partial \theta}, \quad (S13)$$

where  $\eta > 0$  is a viscosity-like coefficient. By dimensional analysis, we can substitute  $\eta$  by  $E \cdot \tau$ , where  $E$  is a characteristic elastic modulus of the cell and  $\tau$  is a phenomenological time constant. This introduces, in a natural manner, an intrinsic timescale to the reorientation process

$$\frac{d\theta}{dt} = -\frac{1}{E \cdot \tau} \cdot \frac{\partial u^{cell}}{\partial \theta}. \quad (S14)$$

On the right hand side of this equation is the configurational force acting on the cell, which is derived from the strain energy pumped into it by the cyclic stretching. The temporal scales involved here depend on the stretching frequency alone (we assume an elastic substrate response). On the left hand side is the cell response to this force, namely rotation. As cell rotation ( $\Delta\theta$ ) takes place through directed formation and disintegration processes of the relevant (cellular) molecular components, the timescales for recruitment of new molecules, or release of resident ones ( $\sim 10s$  [4, 5]) effectively limit the temporal response of the reorientation. Thus, for the relatively rapid stretch frequencies analyzed in this work ( $1/f \leq 1s$ ), the configurational force on the right hand side may be replaced by its time average

$$\frac{d\theta}{dt} = -\frac{1}{E \cdot \tau} \cdot \frac{1}{\xi} \int_0^\xi \frac{\partial u^{cell}}{\partial \theta} dt, \quad (S15)$$

where integration is performed over a characteristic molecular kinetics timescale,  $\xi$  ( $\sim 10s$  for FAs and actin filament networks).

Plugging-in the result for the strain energy density found above (Eq. S9), we obtain

$$\frac{d\theta}{dt} = c \cdot \frac{\frac{1}{\xi} \int_0^\xi \varepsilon_{xx}^2(t) dt}{\tau} \cdot (1+r) \cdot \sin(2\theta) \cdot \left[ \frac{(1+r) \cdot \cos^2(\theta) - 1}{b} + (1-r) \right], \quad (\text{S16})$$

where  $c = \frac{K}{bE}$ . Finally, after substituting  $\varepsilon_{xx}(t)$  according to Eq. S1, we arrive at the expression for the reorientation dynamics, under cyclic stretching, of the joint FA and SF angle,  $\theta$

$$\frac{d\theta}{dt} = \frac{3}{8} \cdot c \cdot \frac{\varepsilon_{xx}^2}{\tau} \cdot (1+r) \cdot \sin(2\theta) \cdot \left[ \frac{(1+r) \cdot \cos^2(\theta) - 1}{b} + (1-r) \right]. \quad (\text{S17})$$

Reorientation thus takes place according to Eq. S17 until reaching one of the two, mirror-image, stable steady state solutions,  $\bar{\theta}_{theory}$ . See figure below for plot of  $\dot{\theta}(\theta)$  at different  $r$  values (Supplementary Fig. 2).

Notes:

1.  $b$  depends on the anisotropic elastic constants of the cell (or relevant parts of it). We can estimate its range of magnitudes by addressing two extreme scenarios. For weak anisotropy, the relations between  $A, B, C$  and  $D$  are similar to that of an isotropic solid. In that case,  $b$  can assume any value. In the other extreme, of strong anisotropy,  $E_{\rho\rho}^{cell} \gg E_{\theta\theta}^{cell}, \mu_{\rho\theta}^{cell}$  and  $\nu_{\theta\rho}^{cell} \nu_{\rho\theta}^{cell} \approx 0$  yield  $b \sim 1$ . In this work we extracted  $b = 1.13 \pm 0.04$ , suggesting that we are close to the strong anisotropy case. The uniformity of  $b$  over different substrate rigidities and cell lines, suggests that the elastic constants  $A, B, C, D$  are an intrinsic property of the cell.
2. For the strong anisotropy case, where  $A \gg (C - 2 \cdot (B + 2D))$ ,  $b$  can be approximated as  $b \approx 1 + \alpha \cdot \frac{E_{\theta\theta}^{cell}}{E_{\rho\rho}^{cell}}$ , where  $\alpha = (\frac{B+2D}{C} - 1)$ . This expression highlights the significance of  $b$ , providing direct comparison of the two orthogonal Young's moduli of the cell:  $E_{\theta\theta}^{cell}$  and  $E_{\rho\rho}^{cell}$ .
3. The value of  $c$  can be estimated in a similar manner to  $b$ . For weak anisotropy, we obtain  $c \sim 0$ , while for strong anisotropy its value should be close to unity,  $c \approx 1$  (where we have also assumed that  $E \sim E_{\rho\rho}^{cell}$ ). In the manuscript, Eq. S17 was used with  $c = 1$  and the extracted  $\tau$  values are therefore correct up to a multiplicative constant of order unity. Moreover, so long as  $b$  remains constant under different experimental conditions and for different cell lines, so should  $c$ , which is a function of the same set of elastic constants ( $A, B, C, D$ ).
4. For the measured  $b = 1.13$  value we obtain from Eq. S10 the following relation between the elastic constants:  $0.13A + 1.13C = 1.26(B + 2D)$ . In addition, as we observe stable steady state solutions for the final orientation angle, the parameter  $K$  must necessarily be positive (see Eq. S9), which translates to  $A > (B + 2D)$  and  $C < (B + 2D)$ . This last result implies that  $E_{\rho\rho}^{cell} > E_{\theta\theta}^{cell}$  ( $A > C$ ) indicating that the rigidity of the cell (or relevant parts of it) is higher along its long axis.
5. While wood is very different from cells (or relevant cell parts) in composition, size and dimensionality ( $3D$  vs  $2D$ ) it is, on the other hand, a well characterized anisotropic material [6]. Calculating the predicted  $b$  value for the elastic constants of 15 different types of hardwoods (where by crude analogy the wood's fibre direction corresponds to the FA and SF  $\rho$  direction), we find an average value of  $b = 1.15$  in surprising similarity with

our own result. The corresponding average  $c$  value for these hardwoods is  $c = 0.83$ , in close agreement with the value used in the manuscript ( $c = 1$ ). In addition, we obtain  $\alpha = 1 - 2$ . As to the relations between the different elastic constants:  $E_{\rho\rho} \approx 10 - 20 \cdot E_{\theta\theta}$ ,  $E_{\rho\rho} \approx 10 - 20 \cdot \mu_{\rho\theta}$ ,  $\nu_{\theta\rho} \approx 0.04$  and  $\nu_{\rho\theta} \approx 0.4$ .

6. The cell body orientation analyzed in the manuscript (for polarized cells only) tracks the dark, actin-rich, cell core. This measure reflects the mean SF angle in that region and was thus analyzed using Eq. S17.
7. SF reorientation is not a process dictated at the cell level, but rather possibly involves smaller parts of it. This is supported by observations of cells, at the end of cyclic stretching experiments, with SFs which are not all oriented in the same direction, but rather along both mirror-image angles (Supplementary Fig. 1b).

## Supplementary Note 2: Constraints and thresholds for the reorientation process

Smooth cell reorientation does not take place under any cyclic stretching conditions. First we observe that the stretch amplitude influences both the rotation time and final angular distribution. The overall rotation duration scales with  $\tilde{\varepsilon}_{xx}^{-2}$  (Eq. S17) and therefore a cell population that requires an hour to reorient under 10% strain is expected to prolong to 100 hours under a 1% stretch. As cultured cells typically divide within 24 hours, this rotation may never complete. Turning to look at the SF angular distribution following cyclic stretching (see e.g. Fig. 1e), we note that the angular distribution width scales with  $\tilde{\varepsilon}_{xx}^{-1}$  (will be shown elsewhere). Consequently, this width will be 10 times larger in the low strain case (presented above) compared to its higher strain counterpart, making it more difficult to discern over the naturally random cell orientations. In addition, we also expect a cell dependant threshold amplitude below which cell sensitivity or molecular “noise” will drown out the external stretch signal. At the other extreme, the elastic response of cells to the applied stretch is limited to a finite amplitude range, beyond which mechanical damage might take place. Finally, as discussed above, the effective strain transferred to the cells depends not only on the amplitude of substrate stretch, but also on the substrate rigidity. Thus the same cyclic matrix strain may drive cell reorientation on one matrix, but have no similar effect on a considerably softer matrix [7].

The relevant molecular kinetic timescales define a transition frequency below which the response to cyclic stretching is greatly attenuated. Above this frequency we expect an intermediate stage where molecular “noise” and high cellular activity (such as high motility) can hinder the reorientation. At frequencies much faster than the molecular kinetic timescales ( $\sim 1Hz$ ), complete reorientation should take place, as discussed in the previous section.

## Supplementary References

- [1] Solon, J., Levental, I., Sengupta, K., Georges, P. C. & Janmey, P. A. Fibroblast Adaptation and Stiffness Matching to Soft Elastic Substrates. *Biophys. J.* **93**, 4453-4461 (2007).
- [2] Lu, L., Oswald, S. J., Ngu, H. & Yin, F. C.-P. Mechanical Properties of Actin Stress Fibers in Living Cells. *Biophys. J.* **95**, 6060-6071 (2008).
- [3] Landau, L. D. & Lifshitz, E. M. *Theory of Elasticity, 3rd ed.*. (Pergamon Press: 1986).
- [4] Wolfenson, H. *et al.* A Role for the Juxtamembrane Cytoplasm in the Molecular Dynamics of Focal Adhesions. *PLoS ONE* **4**, e4304 (2009).
- [5] Fritzsche, M., Lewalle, A., Duke, T., Kruse, K. & Charras, G. Analysis of turnover dynamics of the submembranous actin cortex. *Mol. Biol. Cell* **24**, 757-767 (2013).
- [6] Green D. W., Winandy J. E. & Kretschmann D. E. Mechanical Properties of Wood (Forest Products Laboratory, Eds.). In *Wood Handbook - Wood as an Engineering Material* (U.S. Department of Agriculture: 2001).
- [7] Faust, U. *et al.* Cyclic Stress at mHz Frequencies Aligns Fibroblasts in Direction of Zero Strain. *PLoS ONE* **6**, e28963 (2011).